[12] K. I. Pedersen, G. Monghal, I. Z. Kovács, T. E. Kolding, A. Pokhariyal, F. Frederiksen, and P. Mogensen, "Frequency domain scheduling for OFDMA with limited and noisy channel feedback," in *Proc. IEEE VTC*, Sep. 2007, pp. 1792–1796.

[13] I. Z. Kovács, K. I. Pedersen, T. E. Kolding, A. Pokhariyal, and M. Kuusela, "Effects of non-ideal channel feedback on dual-stream MIMO-OFDMA system performance," in *Proc. IEEE VTC*, Sep. 2007, pp. 1852–1856.

[14] Y. Sun, W. Xiao, R. Love, K. Stewart, A. Ghosh, R. Ratasuk, and B. Classon, "Multi-user scheduling for OFDMA downlink with limited feedback for evolved UTRA," in *Proc. IEEE VTC—Fall*, Sep. 2006, pp. 1–5.

[15] J. Leinonen, J. Hamalainen, and M. Juntti, "Performance analysis of downlink OFDMA frequency scheduling with limited feedback," in *Proc. IEEE ICC*, Jun. 2008, pp. 3318–3322.

[16] Y.-J. Choi and S. Bahk, "Selective channel feedback mechanism for wireless multichannel scheduling," in *Proc. IEEE WoWMoM*, 2006, pp. 289–300.

[17] J. Chen, R. A. Berry, and M. L. Honig, "Performance of limited feedback schemes for downlink with finite coherence time," in *Proc. IEEE ISIT*, Jun. 2007, pp. 2751–2755.

[18] S. Yoon, C. Suh, Y. Cho, and D. Park, "Orthogonal frequency division multiple access with an aggregated sub-channel structure and statistical channel quality measurements," in *Proc. IEEE VTC*, Sep. 2004, pp. 1023–1027.

[19] H. Ekström, A. Furuskär, J. Karlsson, M. Meyer, S. Parkvall, J. Torsner, and M. Wahlqvist, "Technical solutions for the 3G long term evolution," *IEEE Commun. Mag.*, vol. 44, no. 3, pp. 38–45, Mar. 2006.

[20] 3GPP TSG RAN, 25.814, *Physical Layer Aspects for Evolved UTRA (Rel. 7)*, Jun. 2006. Ver. 7.0.0.

[21] M. Dottling, B. Raaf, and J. Michel, "Efficient channel quality feedback schemes for adaptive modulation and coding of packet data," in *Proc. IEEE VTC—Fall*, Sep. 2004, pp. 1243–1247.

[22] H. Asplund, J. Medbo, B. Göransson, J. Karlsson, and J. Sköld, "A simplified approach to applying the 3GPP spatial channel model," in *Proc. IEEE PIMRC*, Sep. 2006, pp. 1–5.

[23] 3GPP contribution R1-063383, *Evaluation Method for Benchmarking CQI Schemes for LTE*, Nov. 2006. [Online]. Available: www.3gpp.org

[24] N. Wei, A. Pokhariyal, C. Rom, B. E. Priyanto, F. Frederiksen, C. Rosa, T. B. Sørensen, T. E. Kolding, and P. E. Mogensen, "Baseline E-UTRA downlink spectral efficiency evaluation," in *Proc. IEEE VTC*, Sep. 2006, pp. 1–5.

[25] 3GPP Technical Specification Group Radio Access Network, 36.211, *Physical Channels and Modulation (Rel. 8)*, Nov. 2007.

[26] K. Brueninghaus, D. Astély, T. Sälzer, S. Visuri, A. Alexiou, S. Karger, and G.-A. Seraji, "Link performance models for system level simulations of broadband radio access systems," in *Proc. IEEE PIMRC*, Sep. 2005, pp. 2306–2311.

[27] D. Chase, "Code combining: A maximum-likelihood decoding approach for combining an arbitrary number of noisy packets," *IEEE Trans. Commun.*, vol. COM-33, no. 5, pp. 385–393, May 1985.

[28] J. Winters, "Optimum combining in digital mobile radio with cochannel interference," *IEEE J. Sel. Areas Commun.*, vol. SAC-2, no. 4, pp. 528–539, Jul. 1984.

[29] A. Pokhariyal, K. I. Pedersen, G. Monghal, I. Z. Kovacs, C. Rosa, T. E. Kolding, and P. E. Mogensen, "HARQ aware frequency domain packet scheduler with different degrees of fairness for the UTRAN long term evolution," in *Proc. IEEE VTC—Spring*, May 2007, pp. 2761–2765.

[30] P. Svedman, L. J. Cimini, and B. Ottersten, "Using unclaimed subcarriers in opportunistic OFDMA systems," in *Proc. IEEE VTC*, Oct. 2006, pp. 1–5.

[31] P. Svedman, D. Hammarwall, and B. Ottersten, "Sub-carrier SNR estimation at the transmitter for reduced feedback OFDMA," in *Proc. Eur. Signal Process. Conf.*, Sep. 2006.

[32] A. Sampath, P. S. Kumar, and J. M. Holtzman, "On setting reverse link target SIR in a CDMA system," in *Proc. IEEE VTC*, May 1997, pp. 929–933.

[33] K. I. Pedersen, F. Frederiksen, T. E. Kolding, T. F. Lootsma, and P. E. Mogensen, "Performance of high speed downlink packet access in co-existence with dedicated channels," *IEEE Trans. Veh. Technol.*, vol. 56, no. 3, pp. 1262–1271, May 2007.

Design and Analysis of Prerake Ultrawideband Impulse Radio (PR-UWB-IR) With Turbo Outer Codes

Usman Riaz, Yu-Hao Chang, and C.-C. Jay Kuo

***Abstract*—The performance of a precoded ultrawideband impulse radio (UWB-IR) system using prerake as the inner code and superorthogonal turbo code (SOTC) or repetition code (RC) as outer codes is investigated in this paper. Prerake UWB-IR transmits information bits with time-reversed channel information. Due to the low transmission power of the UWB-IR, the sequence is repeated through outer coding. The prerake technique demands that the channel information be available to the transmitter. The tradeoff between the feedback channel information and several system performance metrics such as the length of the outer code and bit error rate (BER) is studied. It is shown that there exists a minimum feedback quantity required to achieve a target system performance in different communication scenarios. The optimal quantity of feedback channel knowledge and intersymbol interference (ISI) are investigated and verified by computer simulation.**

***Index Terms*—Asymptotic performance bounds, inner codes, intersymbol interference (ISI), outer codes, repetition codes (RCs), superorthogonal turbo codes (SOTCs), ultrawideband impulse radio (UWB-IR).**

I. Introduction

The prerake technique has been proposed by some researchers to reduce the receiver complexity while accumulating sufficient signal power for ultrawideband impulse radio (UWB-IR) decoding, including prerake diversity combining [1], time-reversal prefiltering (TRP) [2], and channel phase precoding [3]. To explain the prerake idea, we use TRP as an example. In TRP, the information bit is first prefiltered by the time-reversed channel response at every frame, as shown in Fig. 1, which is labeled as the inner code and can be viewed as a special form of the repetition code (RC). Compared with that of the conventional rake receiver without prefiltering [4], the complexity of the prerake receiver is considerably reduced; at the same time, the complexity of the transmitter dramatically increases, and more complex feedback is required. The inner code was adopted in [1], where pulses are transmitted at a very high power level without considering the Federal Communications Commission regulation on the emitted power. However, unlike Imada and Ohtsuki [1], we may treat the inner code as one frame and use the outer code as well to account for the low transmission power of the UWB-IR. This choice leads to the outer code and achieves either RC or low-rate low-complexity superorthogonal turbo code (SOTC).

The performance of a precoded UWB-IR system using prerake as the inner code and SOTC or RC as outer codes is investigated in this paper. The SOTC outer code has a monotonically decreasing bit error rate (BER) as the code rate decreases [5]. Compared with that of conventional turbo codes, its decoding complexity is lower. The prerake system requires the channel information available to the

Manuscript received February 27, 2008; revised October 15, 2008, February 15, 2009, and April 3, 2009. First published May 29, 2009; current version published November 11, 2009. The review of this paper was coordinated by Prof. A. M. Tonello.

The authors are with the Ming Hsieh Department of Electrical Engineering and the Integrated Media Systems Center, University of Southern California, Los Angeles, CA 90089-2564 USA (e-mail: uriaz@usc.edu; yuhaocha@usc.edu; cckuo@sipi.usc.edu).

Color versions of one or more of the figures in this paper are available online at http://ieeexplore.ieee.org.

Digital Object Identifier 10.1109/TVT.2009.2024084

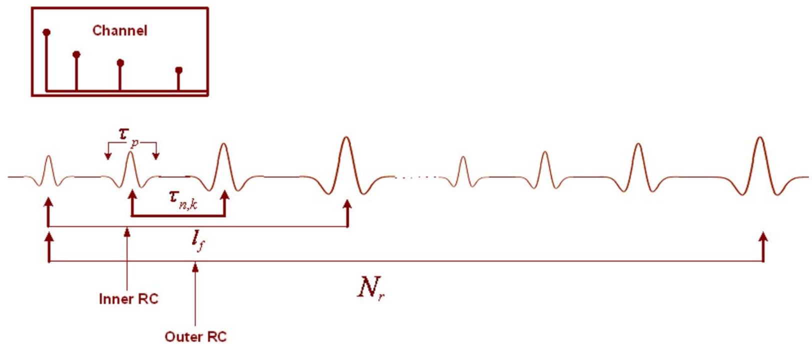

Fig. 1. Inner and outer codes of a transmitted information bit in the PR-UWB-IR system.

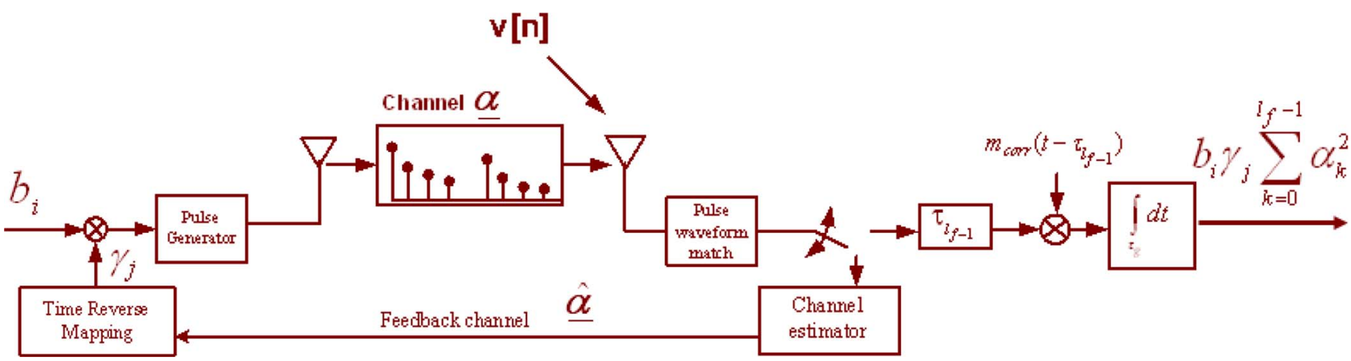

Fig. 2. System block diagram of TRP.

transmitter. Since an UWB-IR channel has a large number of channel taps, it could be expensive for the receiver to send all the estimated channel coefficients to the transmitter through a feedback channel. When only partial channel information is fed back to the transmitter, we may have the selected prerake (SPrerake) scheme and the partial prerake (PPrerake) scheme, as described in [1]. The performance of the coded UWB-IR system depends on the number of feedback channel taps. The tradeoff between the feedback channel information and several system performance metrics such as the length of the outer code and BER is studied. It is shown that there exists a minimum feedback quantity needed to achieve a target system performance (e.g., a targeted BER) in different communication scenarios.

Furthermore, we investigate the intersymbol interference (ISI) effect on system performance with no attempt to equalize the signal. It is also shown that the feedback of more channel taps may not improve the overall system performance since more ISI energy (rather than the useful signal energy) could be accumulated at the receiver output. The problem of selecting the optimal feedback quantity to maximize the output SINR is discussed. In this paper, availability of perfect channel state information is assumed throughout. The bounds are derived in Section III. The effect of ISI on the overall system performance is analyzed in Section IV. The simulation results are shown in Section V. Finally, concluding remarks are given in Section VI.

II. System Model

The signal model for a single-user prerake UWB-IR (PR-UWB-IR) system is presented in this section.

A. Channel Model

In this paper, the UWB IEEE channel model [6], which is a modified form of Saleh-Valenzuela (S-V) [7] has been used. Similar to [8], the channel impulse response can be written in simplified form as

$$h(t)=\sum_{j=1}^{L_{\rm ch}}\alpha_j\delta(t-\tau_j) \tag{1}$$

where the cluster and ray amplitude is represented by the term α_j, both the cluster and ray time delays are captured by delay τ_j, and $L_{\rm ch}$ is the total number of multipaths of all rays and clusters combined. Four different UWB multipath channel models, i.e., CM1–CM4, have been defined, and the corresponding channel parameters are provided in [6]. Similar to [8], the multipaths are assumed to be integral multiples of the minimum time resolution λ.

B. Transmitted Signal

The generic PR-UWB-IR transmitter encodes every information bit based on the time-reversed channel information, which is provided by the receiver to the transmitter through a feedback channel. After precoding, the transmitted signal is of the following form:

$$s(t)=\sqrt{\frac{E_p}{\kappa}}\sum_i b_{\lfloor i/N_r\rfloor}\sum_{j=0}^{l_f-1}\gamma_j p(t-iT_s-\tau_j) \tag{2}$$

where E_p is the energy per pulse, $b_i\in\{1,-1\}$ is the ith binary phase-shift keying signal, γ_j is the time-reversed coded information based on the feedback channel information from the receiver, $\lfloor x\rfloor$ is the floor function of x, and $p(t)$ is a unit-power Gaussian-shaped pulse. The precoding process is shown in Fig. 2.

The energy per bit E_b and the energy per pulse are related via $E_p = E_b/N_r$, where l_f is the number of feedback channel taps, and N_r is the count of the outer code. Furthermore, γ_j and α_j are related via $\gamma_j=\alpha_{l_f-1-j}$ [1], and $\kappa=\sqrt{\sum_{j=0}^{l_f-1}\alpha_j^2}$ is a normalizing factor that is used to ensure that the received signal-to-noise ratio (SNR) in the

PR-UWB-IR system is the same as that of the conventional rake-diversity-combining receiver.

C. Received Signal

The received signal for the information bit with $i = 0$ is given by (3), where $n(t)$ is the Gaussian noise process with zero mean and power spectral density $N_0/2$. The receiver structure in PR-UWB-IR is a simple correlation detector [1]. To extract the peak value of the received signal, the receiver samples at time $(l_f - 1)\lambda$. The equivalent discrete time signal after correlation is given in (4), where $\nu^o_{l_f-1} \sim \mathcal{N}(0, E_p(N_o/2))$, $l + j \leq L_{\mathrm{ch}}$, L_{ch} is the total number of channel taps, and

$$\begin{aligned} r_0(t) =& b_0\sqrt{\frac{E_p}{\kappa}} \sum_{j=0}^{l_f-1} \gamma_{l_f-1-j}\alpha_j p\left(t-(l_f-1)\lambda\right) \\ &+ b_0\sqrt{\frac{E_p}{\kappa}} \sum_{l+j\neq(l_f-1)} \gamma_l\alpha_j p\left(t-(l+j)\lambda\right) \\ &+ \sum_{i\neq 0} b_i\sqrt{\frac{E_p}{\kappa}} \\ &\times \sum_{l,j}\gamma_l\alpha_j p\left(t-iT_s-(l+j)\lambda\right) + n(t). \end{aligned} \tag{3}$$

III. Performance Analysis With Partial Feedback Channel Information

In this section, we analyze the performance of PR-UWB-IR with SOTC as the outer code and the partial yet exact channel information as the inner code. The analysis aims to understand the tradeoff between the BER and the number of feedback channel taps l_f

$$\begin{aligned} r^0_{l_f-1} =& b_0\frac{E_p}{\sqrt{\kappa}} \sum_{j=0}^{l_f-1}\alpha_j^2 + b_0\sqrt{\frac{E_p}{\kappa}} \sum_{l+j\neq(l_f-1)}\gamma_l\alpha_j \\ &\times \left\langle p\left(t-(l+j)\lambda\right), m^0_{\mathrm{corr}}\left(t-(l_f-1)\lambda\right)\right\rangle \\ &+ \sum_{i\neq 0} b_i\sqrt{\frac{E_p}{\kappa}}\sum_{l,j}\gamma_l\alpha_j \\ &\times \left\langle p\left(t-iT_s-(l+j)\lambda\right), m^0_{\mathrm{corr}}\left(t-(l_f-1)\lambda\right)\right\rangle \\ &+ \nu^o_{l_f-1}. \end{aligned} \tag{4}$$

The generic SOTC structure with constituent superorthogonal convolution codes was described in [5] and will subsequently be used in this paper.

A. Performance Analysis in Multipath Channels

The performance of coded PR-UWB-IR systems in the additive white Gaussian noise (AWGN) channel and a realistic multipath channel can be derived by following the approach given in [5] and [9]. Let $\boldsymbol{c}_{(N_{\mathrm{Block}}\times N_r)\times 1}$ be the transmitted coded sequence. The kth time-reversed coded bit at the receiver output is given by

$$r^k_{l_f-1} = c_k\frac{E_p}{\sqrt{\kappa}}\sum_{j=0}^{l_f-1}\alpha_j^2 + \sqrt{E_p}\nu^k_{l_f-1} \tag{5}$$

where $\nu^k_{l_f-1}$ is a zero-mean Gaussian random variable with power spectral density $N_o/2$. The conditional pairwise error probability of a coded sequence in a UWB channel can be derived from (5) and is given by

$$P_e(\boldsymbol{c}_o \rightarrow \boldsymbol{c}_n|\boldsymbol{\alpha}) = Q\left(\sqrt{\frac{2dE_b}{N_o}\frac{1}{N_r}\sum_{j=0}^{l_f-1}\alpha_j^2}\right). \tag{6}$$

The BER upper bound is given by [10]

$$P_e(b|\boldsymbol{\alpha}) \leq \sum_{k=1}^{\lfloor\frac{N}{2}\rfloor}\binom{2k}{k}N^{-1}\frac{\left(Z^{2+2z_{\min}}\right)^k}{\left(1-Z^{\epsilon_m 2^{m-2}}\right)^{2k}} \tag{7}$$

where $Z = P_e(\boldsymbol{c}_o \rightarrow \boldsymbol{c}_n|\boldsymbol{\alpha})$. Hence, (6) can be substituted into (7) to calculate the conditional BER $P_e(b|\boldsymbol{\alpha})$ in a realistic multipath UWB channel for the medium-to-high-SNR regime [9]. On the other hand, for the low-SNR regime, the analysis can be performed using the input–output weight enumerating function of the code [11] and density evolution [12]. The semianalytical bound developed for the uncoded system in [8] can be extended to our coded system. Although the analysis of the proposed prerake SOTC system in a multipath channel is quite involved, we may define the effective SNR as

$$\mathrm{SNR}_{\mathrm{eff}} = \frac{E_b}{N_o}\frac{1}{N_r}\sum_{j=0}^{l_f-1}\alpha_j^2$$

and use it to simplify the analysis. That is, we may treat the proposed PR-UWB-IR system in a multipath channel as the SOTC system in the AWGN channel by setting SNR to $\mathrm{SNR}_{\mathrm{eff}}$. By calculating the conditional error probability $P(b|\boldsymbol{\alpha})_{\mathrm{eff}}$ corresponding to $\mathrm{SNR}_{\mathrm{eff}}$ from the BER curve in the AWGN channel, we can obtain the following semianalytical BER:

$$P_e(b)_{\mathrm{SAB}} = E_{\boldsymbol{\alpha}}\left\{P(b|\boldsymbol{\alpha})_{\mathrm{eff}}\right\}. \tag{8}$$

This bound is tight in the absence of ISI, which will be shown in Section V.

B. Minimum Number of Feedback Channel Taps

The prerake transmitter requires the channel impulse response, which is sent by the receiver through a feedback link. Since the UWB channel contains a large number of multipath components, the feedback of complete channel information could be expensive. On the one hand, it is desirable to reduce the number of feedback channel taps l_f to lower the feedback overhead. On the other hand, a smaller l_f value lowers the received signal power so that we have increased N_r (and, consequently, lowered system throughput) to accumulate enough signal power for a given BER target.

In this section, we study the tradeoff between N_r and l_f with respect to a target error probability $P_e(b)_{\mathrm{target}}$ for both the outer RC and the SOTC cases. Reduction in the feedback overhead achieved by the outer-SOTC-coded P-UWB-IR over the outer RC PR-UWB-IR is demonstrated in *Example 2* of Section V.

1) Outer RC Case: The error probability for the outer RC PR-UWB-IR system (or the time-reversed prefilter system) is given as

$$P_e(b|\boldsymbol{\alpha}) = Q\left(\sqrt{\left(\frac{2E_p}{N_o}\right)N_r\sum_{j=0}^{l_f-1}\alpha_j^2}\right). \tag{9}$$

Due to the lognormal distribution for α_j, it is difficult to find a closed form for $P_e(b)$. Hence, we define the following channel energy-capture function to approximate the signal power collected from those l_f multipath components:

$$g(a_{\mathrm{ch}}, l_f) = \begin{cases} 1 - e^{(-a_{\mathrm{ch}}l_f)} \sim \sum_{j=0}^{l_f-1}\alpha_j^2, & \text{if } l_f > 0 \\ 0, & \text{if } l_f \leq 0 \end{cases} \tag{10}$$

where a_{ch} depends on the channel, i.e., CM1–CM4, mode and the feedback scheme and is calculated for a given channel using exponential curve fitting. We will use $g(a_{\mathrm{ch}}, l_f)$ in subsequent sections to simplify the analysis and show its validity through computer simulation. By substituting the channel energy-capture function in (10) into (9), the number of required channel taps can be calculated by solving

$$Q\left(\sqrt{\frac{2E_p}{N_o}N_r g(a_{\mathrm{ch}}, l_f)}\right) = P_e(b)_{\mathrm{target}}. \tag{11}$$

As a result, we have

$$l_f = -\left(\frac{1}{a_{\mathrm{ch}}}\right) \times \ln\left[1 - \frac{1}{(2E_p/N_o)(N_r)}\left(Q^{-1}\left[P_e(b)\right)_{\mathrm{target}}]\right)^2\right] \tag{12}$$

where Q^{-1} is the inverse of the Q-function.

2) Outer SOTC Case: The l_f value for the outer-SOTC-case PR-UWB-IR system can be derived from the BER based on (7), i.e.,

$$P_e(b|\boldsymbol{\alpha}) \leq \sum_{w=1}^{N} \frac{w}{N} W^w A^{\mathrm{PCC}}(w, Z)|_{Z=P_e(\boldsymbol{c_o}\rightarrow\boldsymbol{c_n}|\boldsymbol{\alpha})} \tag{13}$$

where variable Z can be approximated by

$$Z \approx e^{-\left(\frac{E_p}{N_o}\right)\frac{1}{N_r}g(a_{\mathrm{ch}}, l_f)}. \tag{14}$$

The BER behavior is characterized by the following theorem and corollary:

Theorem 1: Given the AWGN channel, the targeted BER for the medium-to-high-SNR regime can be approximated by

$$\begin{aligned} P_e(b)_{\mathrm{target}} &= \sum_{k=1}^{\lfloor \frac{N}{2} \rfloor} \binom{2k}{k} N^{-1} \frac{(Z^{2+2z_{\min}})^k}{(1 - Z^{\epsilon_m 2^{m-2}})^{2k}} \\ &\approx \frac{2}{N}\left\{\frac{e^{-\frac{E_b}{N_o}\frac{1}{N_r}(2+2z_{\min})}}{\left[1 - e^{-\frac{E_b}{N_o}\frac{1}{N_r}\epsilon_m 2^{m-2}}\right]^2}\right\} \end{aligned} \tag{15}$$

where $Z \approx e^{-(E_b/N_o)(1/N_r)}$.

Proof: See the Appendix. Then, we can extend the result from the AWGN channel in Theorem 1 to the multipath channel using the following corollary:

Corollary 1: Given the multipath channel model in Section II-A, the targeted error probability $P_e(b)_{\mathrm{target}}$ can be found as

$$\begin{aligned} P_e(b)_{\mathrm{target}} &= \sum_{k=1}^{\lfloor \frac{N}{2} \rfloor} \binom{2k}{k} N^{-1} \frac{(Z^{2+2z_{\min}})^k}{(1 - Z^{\epsilon_m 2^{m-2}})^{2k}} \\ &\approx \frac{2}{N}\left\{\frac{e^{-\frac{E_b}{N_o}\frac{1}{N_r}(2+2z_{\min})g(a_{\mathrm{ch}}, l_f)}}{\left[1 - e^{-\frac{E_b}{N_o}\frac{1}{N_r}\epsilon_m 2^{m-2}g(a_{\mathrm{ch}}, l_f)}\right]^2}\right\} \end{aligned} \tag{16}$$

where $Z \approx e^{-(E_b/N_o)(1/N_r)g(a_{\mathrm{ch}}, l_f)}$.

Proof: By manipulating the expression in (31), we can obtain

$$P_e(b)_{\mathrm{target}} = \frac{2}{N}\left\{\frac{\tilde{K}_1}{\tilde{K}_2}\right\}\left\{1 + \sum_{k>1}\binom{2k}{k}\frac{1}{N}\left\{\frac{\tilde{K}_1}{\tilde{K}_2}\right\}^{2k-2}\right\}. \tag{17}$$

Let $\tilde{K}_1 = e^{-(E_b/N_o)(1/N_r)(1+z_{\min})g(a_{\mathrm{ch}}, l_f)}$ and $\tilde{K}_2 = [1 - e^{-(E_b/N_o)(1/N_r)\epsilon_m 2^{m-2}g(a_{\mathrm{ch}}, l_f)}]$. If $g(a_{\mathrm{ch}}, l_f) = 1$, $P_e(b)_{\mathrm{target}}$ converges to (31). If $g(a_{\mathrm{ch}}, l_f) < 1$, we can follow the procedure in deriving (34) and obtain

$$0 < \frac{\tilde{K}_1}{\tilde{K}_2} < 1, \qquad \text{if} \quad l_f \geq l_{\min} \tag{18}$$

where $l_{\min}$ is the minimum number of feedback channel taps for a given channel type. Then, if $l_f \geq l_{\min}$, we can get the following approximation:

$$1 + \sum_{k>1}\binom{2k}{k}\frac{1}{N}\left\{\frac{\tilde{K}_1}{\tilde{K}_2}\right\}^{2k-2} \approx 1$$

and the proof is completed. ■

The $l_{\min}$ of the coded PR-UWB-IR system can be calculated by setting

$$\frac{\left[e^{(1-e^{-a_{\mathrm{ch}}\cdot l_{\min}})}\right]^{-(2+2z_{\min})\frac{E_b}{N_o}\frac{1}{N_r}}}{\left[1 - e^{(1-e^{-a_{\mathrm{ch}}\cdot l_{\min}})}\right]^{(-\epsilon_m 2^{m-2})\frac{E_b}{N_o}\frac{1}{N_r}}} = \sqrt{P_e(b)_{\mathrm{target}}}. \tag{19}$$

With the approximation $e^{(1-e^{-a_{\mathrm{ch}} l_{\min}})} \approx a_1 + b_1 \exp(-c_1 . l_{\min})$ where parameters a_1, b_1, and c_1 can be found by curve fitting, we have the following equality:

$$\frac{\left[a_1 + b_1 e^{(-c_1\cdot l_{\min})}\right]^{-(2+2z_{\min})\frac{E_b}{N_o}\frac{1}{N_r}}}{\left[1 - (a_1 + b_1 e^{(c_1\cdot l_{\min})})^{(-\epsilon_m 2^{m-2})\frac{E_b}{N_o}\frac{1}{N_r}}\right]} = \sqrt{P_e(b)_{\mathrm{target}}} \tag{20}$$

where a_1, b_1, and c_1 in (20) are known constants, depending on the channel type. Finally, $l_{\min}$ can be determined by numerically solving

$$\begin{aligned} &[a_1 + b_1 e^{-c_1\cdot l_{\min}}]^{-(2+2z_{\min})\frac{E_b}{N_o}\frac{1}{N_r}} - \sqrt{P_e(b)_{\mathrm{target}}} \\ &\times \left[1 - \left(a_1 + b_1 e^{c_1\cdot l_{\min}}\right)^{(-\epsilon_m 2^{m-2})}\frac{E_b}{N_o}\frac{1}{N_r}\right] \\ &- \sqrt{P_e(b)_{\mathrm{target}}} = 0. \end{aligned} \tag{21}$$

IV. Performance Analysis in Intersymbol Interference Channels

We can increase the data rate by reducing the frame duration. However, when the duration of channel response $L_{\mathrm{ch}} \cdot \lambda$ exceeds frame duration T_r, the ISI effect shows up at the receiver output. Feeding back more channel taps increases the signal power and the interference power. We show through analysis and computer simulation that there exists an optimum feedback value l_f for ISI channels as well.

The ISI component in the received signal given by (4) is given in

$$r^0_{\mathrm{ISI}} = \frac{\sqrt{E_p}}{\kappa}\sum_{I\neq 0} b_i \sum_{l,j}\gamma_l \alpha_j \big\langle p\,(t - iP\lambda - (l+j)\lambda) \; m^0_{\mathrm{corr}}\,(t - (l_f - 1)\lambda)\big\rangle. \tag{22}$$

Since the valid ISI terms at the receiver output are determined by the following inner product:

$$\big\langle p\,(t - iP\lambda - (l+j)\lambda)\,, m^0_{\mathrm{corr}}\,(t - (l_f - 1)\lambda)\big\rangle = \begin{cases} 1, & \text{if } l = l_f - 1 - j - iP \\ 0, & \text{if } l \neq l_f - 1 - j - iP \end{cases} \tag{23}$$

we can simplify (22) to

$$r_{\mathrm{ISI}}^0 = \frac{\sqrt{E_p}}{\kappa} \sum_{i=1}^{\left\lfloor \frac{L_{\mathrm{ch}}-1-j}{P} \right\rfloor} \sum_{j=0}^{l_f-1} b_i^0 \alpha_k \alpha_{j+iP} + \frac{\sqrt{E_p}}{\kappa} \sum_{i=1}^{\left\lfloor \frac{j}{P} \right\rfloor} \sum_{j=0}^{l_f-1} b_i^0 \alpha_j \alpha_{j-iP} \quad (24)$$

where the first and second terms at the right-hand side correspond to pre- and post-ISI, respectively.

The pre-ISI term due to the jth emitted code for the ith information symbol is $\sum_{i=1}^{\lfloor (l_f-1-j)/P \rfloor} b_i \alpha_j \alpha_{j+iP}$. Similarly, the post-ISI term is $\sum_{i=1}^{\lfloor j/P \rfloor} b_i \alpha_j \alpha_{j-iP}$. Being conditioned on one channel realization, the ISI power is

$$E_{\boldsymbol{b}|\boldsymbol{\alpha}} \left\{ \left(r_{\mathrm{ISI}}^0\right)^2 \right\} = \frac{E_p^2}{\kappa} \sum_{j=0}^{l_f-1} \sum_{i=1}^{\left\lfloor \frac{L_{\mathrm{ch}}-1-j}{P} \right\rfloor} \alpha_j^2 \alpha_{j+iP}^2 + \frac{E_p^2}{\kappa} \sum_{j=0}^{l_f-1} \sum_{i=1}^{\left\lfloor \frac{j}{P} \right\rfloor} \alpha_j^2 \alpha_{j-iP}^2. \quad (25)$$

By the definition of channel energy-capture function in (25), we can rewrite α_{j+iP}^2 and α_{j-iP}^2 in terms of the difference between two energy capture functions as

$$\begin{aligned} \alpha_{j+iP}^2 &= g(a_{\mathrm{ch}}, j+iP) - g(a_{\mathrm{ch}}, j+iP-1) \\ &\triangleq \Delta g(a_{\mathrm{ch}}, j+iP) \quad (26) \\ \alpha_{j-iP}^2 &= g(a_{\mathrm{ch}}, j-iP) - g(a_{\mathrm{ch}}, j-iP-1) \\ &\triangleq \Delta g(a_{\mathrm{ch}}, j-iP) \quad (27) \end{aligned}$$

where $\Delta g(a_{\mathrm{ch}}, l_f)$ is called the differential channel energy-capture function.

By applying the Cauchy–Schwartz inequality to (25) and substituting (26) and (27) into (25), we can rewrite (25) as

$$E_{\boldsymbol{b}} \left\{ \left(r_{\mathrm{ISI}}^0\right)^2 \right\} \leq E_p^2 \sqrt{\sum_{j=0}^{l_f-1} \sum_{i=1}^{\left\lfloor \frac{L_{\mathrm{ch}}-1-j}{P} \right\rfloor} \Delta g^2(a_{\mathrm{ch}}, j+iP)} + E_p^2 \sqrt{\sum_{j=0}^{l_f-1} \sum_{i=1}^{\left\lfloor \frac{j}{P} \right\rfloor} \Delta g^2(a_{\mathrm{ch}}, j-iP)} \quad (28)$$

where, according to (10), $g^2(a_{\mathrm{ch}}, j-iP) = 0$ for $j < iP$. As a result, using (22) and (25) and the approximation $\sqrt{\sum_{j=0}^{l_f-1} \sum_{i=1}^{\lfloor (L_{\mathrm{ch}}-1-j)/P \rfloor} \Delta g^2(a_{\mathrm{ch}}, j+iP)} \approx \sum_{j=0}^{l_f-1} \sum_{i=1}^{\lfloor (L_{\mathrm{ch}}-1-j)/P \rfloor} \times \Delta g(a_{\mathrm{ch}}, j+iP)$, the SINR is given in (29), shown at the bottom of the page. Furthermore, by substituting (26) and (27) into (29) and performing some manipulations, the simplified form of (29) is given in (30), shown at the bottom of the page, where $C_1(P) = (e^{a_{\mathrm{ch}}-1})(e^{-a_{\mathrm{ch}}P}/1 - e^{-a_{\mathrm{ch}}P})$, $C_3(P) = (e^{a_{\mathrm{ch}}-1})(e^{a_{\mathrm{ch}}P}/1 - e^{a_{\mathrm{ch}}P})$, and $C_2(P) = C_3(P)/1 - e^{-a_{\mathrm{ch}}}$. Hence, given (30), we obtain an explicit expression for SINR in terms of l_f, P, and a_{ch}. Finally, the optimal l_f that maximizes the lower bound on the output SINR can be found by numerically solving (30).

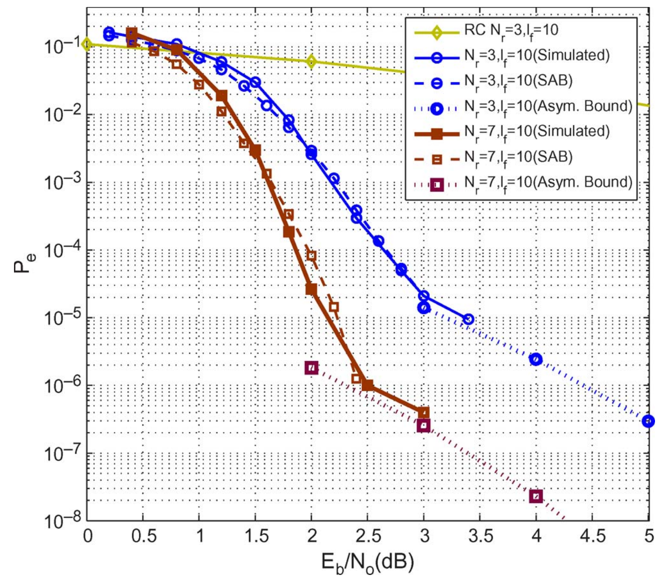

Fig. 3. BER performance of the outer SOTC and RC PR-UWB-IR systems in the CM1 channel with $l_f = 10$, $N_r = 3$, and $N_r = 7$.

V. Computer Simulation

Computer simulation results are given in this section to demonstrate the performance of the proposed PR-UWB-IR system. For SOTC decoding, the suboptimal max-log maximum *a posteriori* (MAP) decoding was adopted, instead of the MAP decoding scheme, which has a much higher complexity. Simulations were performed with a random interleaver of size $N = 1024$ with four iterations. Perfect channel information was assumed to be available at the transmitter. The average BER was evaluated by averaging over 1000 realizations for a given E_b/N_o. The BER simulated performance was compared with the derived semianalytical bound in the low-SNR regime and the asymptotic bounds in the medium-to-high-SNR regime, i.e., $(E_b/N_0 > 2.5$ dB), as shown in Fig. 3. The asymptotic bounds were derived based on MAP

$$\mathrm{SINR}(l_f) \geq \frac{g(a_{\mathrm{ch}}, l_f)}{\frac{N_o}{2E_p} + \sum_{j=0}^{l_f-1} \sum_{i=1}^{\left\lfloor \frac{L_{\mathrm{ch}}-1-j}{P} \right\rfloor} \Delta g(a_{\mathrm{ch}}, j+iP) + \sum_{j=0}^{l_f-1} \sum_{i=1}^{\left\lfloor \frac{j}{P} \right\rfloor} \Delta g(a_{\mathrm{ch}}, j-iP)} \quad (29)$$

$$\mathrm{SINR}(l_f) \geq \frac{g(a_{\mathrm{ch}}, l_f)}{\frac{N_o}{2} + C_1(P) g(a_{\mathrm{ch}}, l_f) + C_2(P) e^{-a_{\mathrm{ch}} l_f} \left(e^{a_{\mathrm{ch}}(l_f - iP)} e^{-a_{\mathrm{ch}}} - 1 \right) + C_3(P)(l_f - iP - 1)} \quad (30)$$

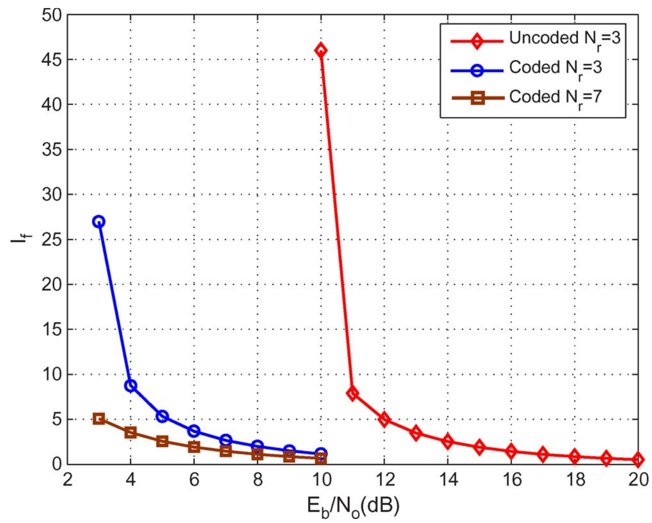

Fig. 4. Comparison of the minimum number of feedback channel taps for the outer SOTC and RC PR-UWB-IR systems in the CM1 Channel with target BER equal to 10^{-6}.

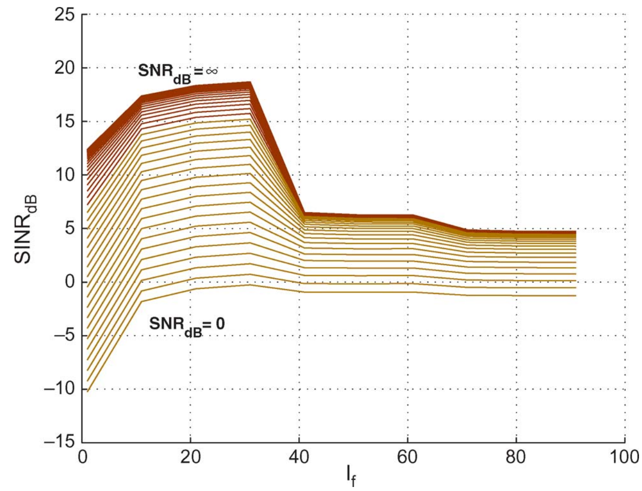

Fig. 5. SINR value as a function of the number of feedback channel taps for the CM3 channel with $P = 30$ and $L_{\text{ch}} = 120$.

decoding and the uniform interleaver assumption [10]. Among various channel modes, only CM1 and CM3 were used in the simulation setup with multipath resolution equal to $\lambda = 0.7$ ns.

Example 1—Comparison of Feedback Overhead: We examine the tradeoff between feedback overhead l_f and the system performance in both the outer SOTC and RC systems in this example. The CM1 channel model was used, and the target BER was set to 10^{-6}. The required minimum channel taps for feedback, as calculated by (12) and (21) for the outer RC and SOTC PR-UWB-IR systems, respectively, are shown in Fig. 4 with different N_r and SNR values.

It is observed that approximately 6 dB more power is required for the outer RC system to get the same BER, compared with the outer SOTC system for a given l_f using $N_r = 3$. The difference in feedback overhead reduction between two coded systems (i.e., $N_r = 3$ and $N_r = 7$ in the given example) for a given l_f is much less, compared with that between the outer SOTC $N_r = 3$ and outer RC $N_r = 3$ systems. In other words, increasing N_r to go beyond 3 for the coded system starts to give a diminishing return in feedback overhead reduction at the cost of higher complexity. Although additional frames can be utilized to boost the received signal power, this choice can, however, lead to throughput degradation, i.e.,

$$P_e(b)_{\text{target}} = \frac{2}{N}\left\{\frac{e^{-\frac{E_b}{N_o}\frac{1}{N_r}(2+2z_{\min})}}{\left[1-e^{-\frac{E_b}{N_o}\frac{1}{N_r}\epsilon_m 2^{m-2}}\right]^2}\right\} + \sum_{k\neq 1}\binom{2k}{k}\frac{1}{N}\left\{\frac{e^{-\frac{E_b}{N_o}\frac{k}{N_r}(2+2z_{\min})}}{\left[1-e^{-\frac{E_b}{N_o}\frac{1}{N_r}\epsilon_m 2^{m-2}}\right]^{2k}}\right\}. \quad (31)$$

Example 2—Impact of the ISI Effect on System Performance: Given a certain channel type, symbol duration T_s, noise power, and perfect channel estimation, the optimal feedback length l_f^* in the presence of ISI and without any channel equalization can be obtained by numerically solving (30). The plot of SINR versus l_f in the CM3 channel with $P = 30$ and $L_{\text{ch}} = 120$ is shown in Fig. 5. Recall that L_{ch} is the total number of channel taps, whereas P is the number of discrete time units of length λ between two successive symbols. It is observed that increasing l_f results in the increase in SINR until the optimal l_f is reached. To feed more channel information back actually results in performance degradation. This is due to the ISI energy present in each channel tap. As more channel taps are accumulated to gather more energy, the ISI effect increases. It is also observed that an increased SNR value results in an increase in SINR. However, as SNR $\to \infty$, the SINR value becomes saturated and upper bounded by approximately 20 dB. This is also due to the ISI effect.

VI. Conclusion

The time-reversed channel impulse response has been used as the inner code, whereas SOTC has been adopted as the outer code in the PR-UWB-IR system in this paper. The SOTC scheme has low decoding complexity and low overhead rate; therefore, it is attractive for low-complexity applications. We have shown that SOTC significantly enhances BER performance while reducing the feedback overhead over the conventional RC via mathematical analysis and computer simulations. In particular, the relationship between the inner code length and the outer code has extensively been investigated. Finally, the ISI effect has been analyzed in terms of SINR without any equalization attempt. The feedback of more channel information may lead to more interference, thus degrading system performance. The optimal feedback overhead that maximizes the SINR value in the presence of ISI has been studied.

Appendix

The bound on the target BER based on (7) can be written as (31). To prove Theorem 1, we need to show that the second term at the right-hand side of (31) is very small, i.e.,

$$\sum_{k\neq 1}\binom{2k}{k}\frac{1}{N}\left\{\frac{e^{-\frac{E_b}{N_o}\frac{k}{N_r}(2+2z_{\min})}}{\left[1-e^{-\frac{E_b}{N_o}\frac{1}{N_r}\epsilon_m 2^{m-2}}\right]^{2k}}\right\} = \sum_{k\neq 1}\binom{2k}{k}\frac{1}{N}\left(\frac{K_1}{K_2}\right)^{2k} \approx 0 \quad (32)$$

where $K_1 = e^{-(E_b/N_o)(1/N_r)(1+z_{\min})}$, and $K_2 = [1 - e^{-(E_b/N_o)(1/N_r)\epsilon_m 2^{m-2}}]$. Using the relation

$$z_{\min} = d_{\text{free-eff}} - 2 = 2^m + 2^{m-2}\epsilon_m - 2$$

K_2 can be expressed in terms of $z_{\min}$ as

$$K_2 = 1 - e^{-\frac{E_b}{N_o}\frac{1}{N_r} z_{\min}} \cdot e^{-\frac{E_b}{N_o}\frac{1}{N_r}(2-2^m)}. \tag{33}$$

Hence, the ratio between K_1 and K_2 can be expressed and simplified as

$$\frac{K_1}{K_2} = \frac{1}{e^{\frac{E_b}{N_o}\frac{1}{N_r}(2^m-1)}\left[e^{(\epsilon_m 2^{m-2}-1)} - 1\right]}.$$

As (34), shown below, implies, K_1/K_2 becomes much smaller when $m \geq 2$ and E_b/N_0 is in the medium-to-high-SNR range. Consequently, we have

$$\sum_{k\neq 1} \binom{2k}{k} \frac{1}{N} \left\{ \frac{e^{-\frac{E_b}{N_o}\frac{k}{N_r}(2+2z_{\min})}}{\left[1 - e^{-\frac{E_b}{N_o}\frac{1}{N_r}\epsilon_m 2^{m-2}}\right]^{2k}} \right\} \approx 0. \tag{34}$$

■

REFERENCES

[1] S. Imada and T. Ohtsuki, "Prerake diversity combining for UWB systems in IEEE 802.15 UWB multipath channel," in *Proc. IWUWBS*, May 2004, pp. 236–240.

[2] T. Strohmer, M. Emami, J. Hansen, G. Papanicolaous, and A. J. Paulraj, "Application of time-reversal with MMSE equalization to UWB communications," in *Proc. IEEE GLOBECOM*, Nov. 2004, vol. 5, pp. 3123–3127.

[3] Y.-H. Chang, S.-H. Tsai, X. Yu, and C.-C. J. Kuo, "Design and analysis of channel-phase-precoded ultra wideband (CPPUWB) systems," in *Proc. IEEE WCNC*, Apr. 2006, pp. 866–871.

[4] M. Z. Win and R. A. Scholtz, "On the energy capture of ultrawide bandwidth signals in dense multipath environments," *IEEE Commun. Lett.*, vol. 2, no. 9, pp. 245–247, Sep. 1998.

[5] P. Komulainen and K. Pehkonen, "A low complexity superorthogonal turbo-code for CDMA applications," in *Proc. IEEE PIMRC*, Taipei, Taiwan, Feb. 1996, vol. 2, pp. 369–373.

[6] *Channel Modelling Sub-Committee, Final Report*, Feb. 2003. IEEE 802.15.SG3a, IEEE P802.15-02/490r1-SG3.

[7] A. Saleh and R. Valenzuela, "A statistical model for indoor multipath propagation," *IEEE J. Sel. Areas Commun.*, vol. SAC-5, no. 2, pp. 128–137, Feb. 1987.

[8] A. Rajeswaran, V. S. Somayazulu, and J. R. Foerster, "RAKE performance for a pulse based UWB system in a realistic UWB indoor channel," in *Proc. ICC*, May 2003, vol. 4, pp. 2879–2883.

[9] U. Riaz, M.-O. Pun, and C.-C. J. Kuo, "Performance analysis of ultra-wide band impulse radio (UWB-IR) with super-orthogonal turbo codes (SOTC)," in *Proc. IEEE Globecom*, San Francisco, CA, Nov. 2006, pp. 981–985.

[10] P. Komulainen and K. Pehkonen, "Performance evaluation of super-orthogonal turbo codes in AWGN and flat Rayleigh fading channels," *IEEE J. Sel. Areas Commun.*, vol. 16, no. 2, pp. 196–205, Feb. 1998.

[11] D. Divsalar, "A simple tight bound on error probability of block codes with application to turbo codes," Jet Propuls. Lab., California Inst. Technol., Pasadena, CA, pp. 42–139, TMO Progress Rep. 42-139, Nov. 1999.

[12] D. Divsalar, S. Dolinar, and F. Pollara, "Iterative turbo decoder analysis based on density evolution," *IEEE J. Sel. Areas Commun.*, vol. 19, no. 5, pp. 891–907, May 2001.

EXIT-Chart-Aided Three-Stage Concatenated Ultrawideband Time-Hopping Spread-Spectrum Impulse Radio Design

R. A. Riaz, R. G. Maunder, M. F. U. Butt,
S. X. Ng, S. Chen, and L. Hanzo

***Abstract*—A serially concatenated and iteratively decoded Irregular Variable-Length Coding (IrVLC) scheme is amalgamated with a unity-rate precoded time-hopping (TH) pulse-position-modulation (PPM)-aided ultrawideband (UWB) spread-spectrum (SS) impulse radio design. The proposed design is capable of operating at low SNRs in Nakagami-m fading channels contaminated by partial band noise jamming (PBNJ) as a benefit of lossless IrVLC joint source and channel coding. Although this scheme may readily be used for lossless video or audio compression, for example, we only used it here for lossless near-capacity data transmission. A number of component variable-length-coding (VLC) codebooks having different coding rates are utilized by the IrVLC scheme for encoding specific fractions of the input source symbol stream. EXtrinsic Information Transfer (EXIT) charts are used to appropriately select these fractions to shape the inverted EXIT curve of the IrVLC and, hence, to match that of the inner decoder, which allows us to achieve an infinitesimally low bit error ratio (BER) at near-capacity SNR values.**

***Index Terms*—EXIT charts, impulse radio, irregular code design, spread-spectrum communications, three-stage concatenated iterative detection, time-hopping, ultrawideband, ultrawideband systems, unity-rate codes, variable-length codes.**

I. INTRODUCTION

The novel contribution of this paper is that we advance the design of time-hopping pulse-position-modulation ultrawideband (TH-PPM-UWB) systems with the aid of sophisticated channel coding in the interest of approaching attainable capacity. More specifically, our TH-PPM-UWB design exploits that, analogous to irregular convolutional coding [1], the family of Irregular Variable-Length Codes (IrVLCs) [2] employs a number of component variable-length-coding (VLC) codebooks having different coding rates [3] for encoding particular fractions of the input source symbol stream. The appropriate lengths of these fractions may be chosen with the aid of EXtrinsic Information Transfer (EXIT) charts [4] to shape the inverted EXIT curve of the IrVLC codec to ensure that it does not cross the EXIT curve of the inner channel codec. This way, an open EXIT chart tunnel may be created even at near-capacity values of SNR.

UWB communications systems are commonly defined as systems that have either more than 20% relative bandwidth compared with the band's center frequency or more than 500-MHz absolute bandwidth. The pioneering work of Win and Scholtz [5]

Manuscript received June 15, 2009; revised June 23, 2009. First published June 23, 2009; current version published November 11, 2009. This work was supported by the Engineering and Physical Sciences Research Council, U.K., under the EU Optimix project.

R. A. Riaz and M. F. U. Butt are with the School of Electronics and Computer Science, University of Southampton, SO17 1BJ Southampton, U.K., and also with the Department of Electrical Engineering, COMSATS Institute of Information Technology, Islamabad 44000, Pakistan (e-mail: rar06r@ecs.soton.ac.uk; mfub06r@ecs.soton.ac.uk).

R. G. Maunder, S. X. Ng, S. Chen, and L. Hanzo are with the School of Engineering and Computer Science, University of Southampton, SO17 1BJ Southampton, U.K. (e-mail: rm@ecs.soton.ac.uk; sxn@ecs.soton.ac.uk; sqc@ecs.soton.ac.uk; lh@ecs.soton.ac.uk).

Digital Object Identifier 10.1109/TVT.2009.2025857